Plant Biotechnology Journal
Open Access

Plant Biotechnology Journal (2025) **23**, pp. 4930–4932 doi: 10.1111/pbi.70254

Brief Communication

Comparative genomics-driven design of virus-delivered short RNA inserts triggering robust gene silencing

Arcadio García[1], Verónica Aragonés[1], Silvia Gioiosa[2], Francisco J. Herraiz[3], Paloma Ortiz-García[1], Jaime Prohens[3], José-Antonio Daròs[1] and Fabio Pasin[1,4,*]

[1]*Instituto de Biología Molecular y Celular de Plantas (IBMCP), Consejo Superior de Investigaciones Científicas – Universitat Politècnica de València (CSIC-UPV), Valencia, Spain*

[2]*Super Computing Applications and Innovation Department, CINECA, Rome, Italy*

[3]*Instituto de Conservación y Mejora de la Agrodiversidad Valenciana (COMAV), Universitat Politècnica de València, Valencia, Spain*

[4]*Centro de Investigaciones Biológicas Margarita Salas (CIB), Consejo Superior de Investigaciones Científicas (CSIC), Madrid, Spain*

Received 22 February 2025;
revised 20 May 2025;
accepted 27 June 2025.
**Correspondence* (Tel +34 918373112; email f.pasin@csic.es)

Keywords: virus-induced gene silencing (VIGS), tobacco rattle virus (TRV), functional genomics, *Nicotiana benthamiana*, *Solanum aethiopicum*, underutilized crops.

RNA products and RNA virus-based technologies have the potential to transform agriculture by enabling on-demand crop trait reprogramming and effective pest and disease management (Pasin *et al*., 2024; Rössner *et al*., 2022). In virus-induced gene silencing (VIGS), engineered RNA viruses can redirect the host RNA interference machineries to target gene silencing through the production of gene-specific small RNAs (sRNAs) (Rössner *et al*., 2022). Although endogenous sRNAs and those resulting from VIGS are in the 20–30-nt range, VIGS vectors are engineered to deliver larger inserts of 200–400 nt with homology to a target gene, often located in less conserved regions to ensure specificity (Ahmed *et al*., 2020). Reducing insert sizes, may enhance the VIGS scalability and applicability to non-model species.

Nicotiana benthamiana is the most widely used model for optimizing VIGS protocols. However, this host has a complex, allotetraploid genome with functionally redundant homeologous gene pairs, and for which no high-quality assemblies were available until very recently (Ranawaka *et al*., 2023). Multi-gene CRISPR-Cas9 mutagenesis was applied to tackle functional redundancy in plants (Berman *et al*., 2025; Ellison *et al*., 2020). Here, we hypothesized that VIGS insert sizes could be lowered to match those of endogenous sRNAs by combining enhanced genomics and transcriptomics resources to guide the design of virus-delivered short RNA inserts (vsRNAi) for simultaneous targeting of homeologous gene pairs.

We focused on the magnesium protoporphyrin chelatase subunit I (*CHLI*) gene, whose downregulation results in leaf yellowing due to a reduction of chlorophyll biosynthesis and levels. Tomato (*Solanum lycopersicum*) is a diploid relative of *N. benthamiana* with high-quality genome assembly and annotation. The tomato *CHLI* coding sequence (CDS) is distributed across three exons with boundaries supported by transcriptomic expression analysis (Supporting experimental procedures). Analysis of reported *N. benthamiana* Niben101 and Niben261 annotations, however, revealed *CHLI* variation including large sequence deletion and insertion, not supported by results obtained by *de novo* transcriptome assembly (Figure S1). A high-quality chromosome-level genome assembly was recently reported for *N. benthamiana* (Ranawaka *et al*., 2023). Sequence searches using the tomato CHLI protein identified homologue loci in chromosomes 5 (NbLab360C05) and 10 (NbLab360C10), whose expression and gene structures were validated by mapping sequencing reads from RNA samples. Leveraging this curated annotation, vsRNAi were designed to target CDS regions conserved in *N. benthamiana* and tomato *CHLI* (Figure S1).

Custom-synthesized DNA oligonucleotide pairs spanning vsRNAi sequences were inserted into pLX-TRV2 of the JoinTRV vector system, which is based on tobacco rattle virus (TRV) (Aragonés *et al*., 2022), by one-step digestion-ligation reactions (Figure 1a). JoinTRV derivatives with 32-, 28-, 24- and 20-nt inserts targeting *CHLI* (vCHLI, vCHLI-28, vCHLI-24 and vCHLI-20, respectively) were inoculated to *N. benthamiana*. After 10 days, upper uninoculated leaves of plants treated with vCHLI, vCHLI-28 and vCHLI-24 showed a yellowing phenotype. Fluorometry revealed a significant reduction of chlorophyll levels in vCHLI ($\bar{x}$ = 0.11), vCHLI-28 ($\bar{x}$ = 0.23) and vCHLI-24 ($\bar{x}$ = 0.39) compared with controls ($\bar{x}$ = 1.00; Figure 1a) and a significant positive correlation with *CHLI* transcript levels measured by RT-qPCR (Figure S2).

Silencing phenotypes of vCHLI-treated plants were robust and equivalent to those obtained by using a VIGS vector including a 300-nt *CHLI* cDNA fragment (Figure S3). Transcriptomes of plants inoculated with the unmodified JoinTRV (CTRL) or its vCHLI derivative were analysed. Abundance of over 4000 transcripts was significantly altered in the vCHLI/CTRL comparison (FDR <0.05; Figures 1b and S4; Data S1 and S2). Transcriptome-wide functional analysis revealed an enrichment of gene ontology terms associated with light responses, and biological processes involved in carbohydrate metabolism, cellulose biosynthesis and cell wall biogenesis (Figure S4c; Data S3–S5), consistent with the anticipated reduction of cell photosynthetic capacity caused by the *CHLI* downregulation.

Among downregulated transcripts, we identified the *CHLI* homeologues (NbL05g17570.1, and NbL10g22050.1; log2(FC) ≤ -1.92, FDR <0.05) and confirmed a global expression reduction of their genomic loci beyond the 32-nt region targeted by vCHLI (Figure 1b; Data S6). Viral amplification of large VIGS inserts can lead to overestimation of expression levels of homologous host genes (Figures S5 and S6); by contrast, vsRNAi enable transcriptome-wide quantification of target gene silencing.

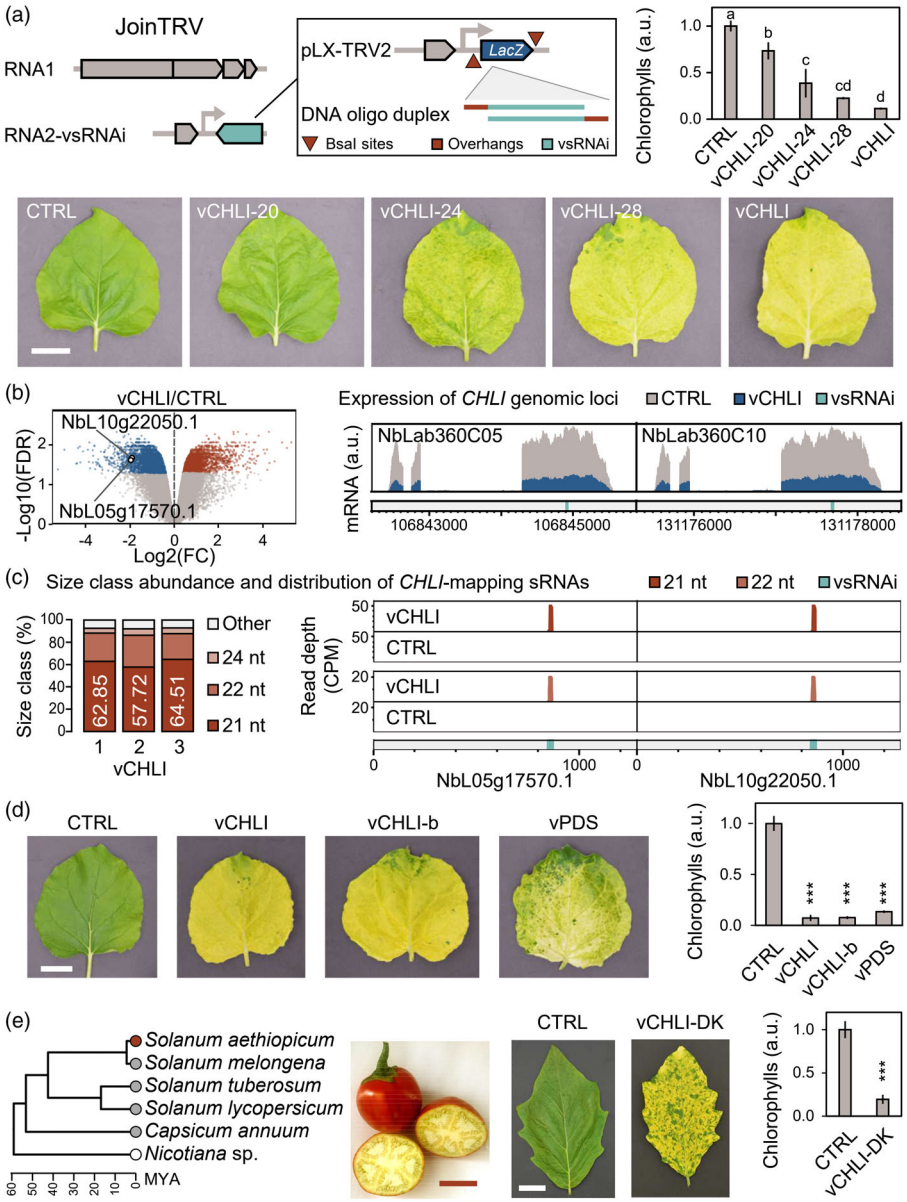

Figure 1 Virus-delivered short RNA inserts (vsRNAi) trigger gene silencing. (a) JoinTRV vector assembly and delivery of 32-, 28-, 24- and 20-nt vsRNAi targeting the two *N. benthamiana CHLI* homeologues (vCHLI, vCHLI-28, vCHLI-24 and vCHLI-20). Leaf phenotypes and chlorophyll levels (mean ± SD, $n = 3$) are shown; CTRL—control. Different letters indicate significant differences ($P < 0.05$), by one-way ANOVA and Tukey's honestly significant difference (HSD) test. (b) Transcriptomics of vCHLI and CTRL samples ($n = 3$) detects a significant downregulation of *CHLI* expression (FDR <0.05). (c) In vCHLI samples, small RNA sequencing shows predominance of 21- and 22-nt sRNAs mapping to *CHLI*, and with a read depth peak (mean, $n = 3$) localized to the vsRNAi-targeted region. (d) Leaf phenotypes and chlorophyll levels (mean ± SD, $n = 3$) are shown for vCHLI-b and vPDS, targeting *CHLI* and *PDS* homeologues, respectively; ***, $P < 0.001$, Student's *t*-test. (e) vsRNAi portability to scarlet eggplant (*Solanum aethiopicum*). Phylogeny and fruits are shown, alongside leaf phenotypes and chlorophyll levels (mean ± SD, $n = 3$) of 'Rossa di Rotonda' plants treated with vCHLI-DK, a pTRV1 + pTRV2 derivative targeting *CHLI*; ***, $P < 0.001$, Student's *t*-test.

We next sequenced sRNAs to assess if their production is involved in the vCHLI-induced phenotypic and transcriptomic changes. In vCHLI samples, vsRNAi triggered host-derived production of sRNAs (Figure S7) and a marked enrichment of sRNAs mapping to *CHLI* transcripts (Figure S8; Data S7 and S8). 21-nt sRNAs were predominant, followed by 22-nt sRNAs (Figure 1c; Data S9), and their levels showed a significant negative correlation with those of *CHLI* transcripts (Figure S9). The vsRNAi-targeted region of *CHLI* transcript sequences exhibited a localized accumulation of 21- and 22-nt sRNAs in vCHLI samples, which was absent in control samples (Figure 1c; Data S10). We concluded that vsRNAi trigger target gene downregulation through region-specific enrichment of 21- and 22-nt sRNAs, known end products of Dicer-like 4 (DCL4) and DCL2, respectively (Rössner *et al*., 2022).

We used vCHLI-b and vPDS to target a second 32-nt region conserved in *CHLI* homeologues or 32-nt of the *PHYTOENE DESATURASE* (*PDS*) gene pair, respectively. In the upper uninoculated leaves of treated plants, we observed a reduction in green pigmentation and chlorophyll levels (Figure 1d),

confirming the broad applicability of vsRNAi for *N. benthamiana* gene functional characterization.

We next assessed vsRNAi portability to crops. The vCHLI insert is conserved in tomato *CHLI* (Figure S1); 'Moneymaker' seedlings inoculated with vCHLI showed leaf yellowing and a significant reduction of chlorophyll levels compared with control plants (Figure S10a). Scarlet eggplant (*Solanum aethiopicum*; Figure 1e) is an underutilized solanaceous crop (Gramazio *et al.*, 2016). Searches of *de novo* assembled transcriptomes and of a genomic assembly (Benoit *et al.*, 2025) confirmed that the 32-nt insert of vCHLI is conserved in scarlet eggplant *CHLI* (100% identity) (Figure S10b). Seedlings of the ecotype 'Rossa di Rotonda' inoculated with vCHLI showed leaf yellowing and a significant reduction of chlorophyll levels compared with control plants (Figure S10b). Using vCHLI-DK, a derivative of the pTRV1 plus pTRV2 vector system used for VIGS and genome editing (Ellison *et al.*, 2020), we delivered a *CHLI*-targeting 32-nt vsRNAi and obtained equivalent results (Figures 1e and S10c), highlighting the versatility of our approach.

Overall, our results demonstrate that vsRNAi as short as 24 nt can effectively produce phenotypic alterations. Use of 32-nt vsRNAi results in robust gene silencing phenotypes, informative transcriptome-wide changes and target transcript downregulation linked to gene-specific production of 21- and 22-nt sRNAs.

Viral delivery of artificial micro-RNAs or trans-acting small interfering RNAs reduces VIGS insert sizes and off-targets (Cisneros *et al.*, 2025). vsRNAi offer equivalent specificity and greatly simplifies viral vector engineering by eliminating intermediate cloning steps and precursor elements required to activate sRNA production. Simplified cloning of vsRNAi fragments, which are nearly 10-fold smaller than those of conventional VIGS and can be synthesized at low cost, may enable high-throughput functional genomics in model plants and crops that contribute food security and on-demand alteration of crop traits.

Acknowledgements

This work was supported by RYC2023-045411-I, FPU20/05477 and PID2023-146418OB-I00 from Ministerio de Ciencia, Innovación y Universidades (Spain) through the Agencia Estatal de Investigación and PROMETEO CIPROM/2022/21 from Generalitat Valenciana. F.P. gratefully acknowledges the grants MiniVi (ELIXIR-IIB, Cineca, Italy) and BCV-2023-1-0021 (Red Española de Supercomputación, Spain), and resources provided by Centro de Supercomputación de Galicia (CESGA, Spain). We thank C. Mallor Giménez (BGHZ-CITA, Spain) for *S. aethiopicum* seeds.

Author contributions

F.P. conceived the study; J.-A.D. and F.P. obtained funding and computational resources; A.G. and F.P. designed experiments with input from the other authors; A.G., V.A., P.O.-G. and F.P. performed the experiments; F.J.H. and J.P. provided materials; A.G., S.G. and F.P. analysed and managed data. F.P. wrote the manuscript with input from A.G. and the other authors; all authors revised and approved the final version.

Conflict of interest

The authors declare no competing interests.

Data availability statement

Supplemental information accompanies this article. The transcriptomic and small RNA sequencing datasets generated are deposited under NCBI BioProject PRJNA1217923. pLX-TRV2-vCHLI is available at Addgene (239842, https://www.addgene.org/239842/).

References

Ahmed, F., Senthil-Kumar, M., Dai, X., Ramu, V.S., Lee, S., Mysore, K.S. and Zhao, P.X. (2020) *pssRNAit*: a web server for designing effective and specific plant siRNAs with genome-wide off-target assessment. *Plant Physiol.* **184**, 65–81.

Aragonés, V., Aliaga, F., Pasin, F. and Daròs, J.A. (2022) Simplifying plant gene silencing and genome editing logistics by a one-*Agrobacterium* system for simultaneous delivery of multipartite virus vectors. *Biotechnol. J.* **17**, e2100504.

Benoit, M., Jenike, K.M., Satterlee, J.W., Ramakrishnan, S., Gentile, I., Hendelman, A., Passalacqua, M.J. *et al.* (2025) *Solanum* pan-genetics reveals paralogues as contingencies in crop engineering. *Nature* **640**, 135–145.

Berman, A., Su, N., Li, Z., Landau, U., Chakraborty, J., Gerbi, N., Liu, J. *et al.* (2025) Construction of multi-targeted CRISPR libraries in tomato to overcome functional redundancy at genome-scale level. *Nat. Commun.* **16**, 4111.

Cisneros, A.E., Alarcia, A., Llorens-Gámez, J.J., Puertes, A., Juárez-Molina, M., Primc, A. and Carbonell, A. (2025) Syn-tasiR-VIGS: virus-based targeted RNAi in plants by synthetic trans-acting small interfering RNAs derived from minimal precursors. *Nucleic Acids Res.* **53**, gkaf183.

Ellison, E.E., Nagalakshmi, U., Gamo, M.E., Huang, P.J., Dinesh-Kumar, S. and Voytas, D.F. (2020) Multiplexed heritable gene editing using RNA viruses and mobile single guide RNAs. *Nat. Plants* **6**, 620–624.

Gramazio, P., Blanca, J., Ziarsolo, P., Herraiz, F.J., Plazas, M., Prohens, J. and Vilanova, S. (2016) Transcriptome analysis and molecular marker discovery in *Solanum incanum* and *S. aethiopicum*, two close relatives of the common eggplant (*Solanum melongena*) with interest for breeding. *BMC Genomics* **17**, 300.

Pasin, F., Uranga, M., Charudattan, R. and Kwon, C.T. (2024) Engineering good viruses to improve crop performance. *Nat. Rev. Bioeng.* **2**, 532–534.

Ranawaka, B., An, J., Lorenc, M.T., Jung, H., Sulli, M., Aprea, G., Roden, S. *et al.* (2023) A multi-omic *Nicotiana benthamiana* resource for fundamental research and biotechnology. *Nat. Plants* **9**, 1558–1571.

Rössner, C., Lotz, D. and Becker, A. (2022) VIGS goes viral: how VIGS transforms our understanding of plant science. *Annu. Rev. Plant Biol.* **73**, 703–728.

Supporting information

Additional supporting information may be found online in the Supporting Information section at the end of the article.

Table S1–S6.
Figure S1–S10.
Data S1–S12.